Transport in Porous Media **26:** 133–146, 1997.

A Directed Percolation Model for Clogging in a Porous Medium with Small Inhomogeneities

C. KAISER
Commission of the European Communities, Joint Research Centre, T.P. 250, I-21020 Ispra (Va), Italy. e-mail: christian.kaiser@jrc.it

(Received: 14 December 1995; in final form: 10 September 1996)

Abstract. We propose a microscopic model based on directed percolation for the process of mechanical clogging of a porous medium by particles suspended in a fluid flow. Under appropriate conditions the deposited particles may form fractal clusters. A criterion for the occurrence of fractal clogging is presented. It links together the particle size and the pore size distribution. The effect of microscopic inhomogeneities is studied inside and outside the critical region using Monte Carlo calculations in two dimensions. The critical exponents remain unchanged because the perturbation induced by these inhomogeneities is irrelevant. The percolation threshold is found to shift to higher values almost linearly with increasing size of obstacles. For size distributed obstacles the arithmetic mean of the distribution is the only significant parameter which determines the shift. Type and broadness of the distribution have no influence. Also the percolation probability depends only on the mean even outside the critical region for all values of the occupation probability. Occupying the same fraction of the porous matrix, large obstacles cause more particles to deposit than small ones.

Key words: fractal pore clogging, directed percolation, inhomogeneous porous medium, Monte Carlo simulations, percolation threshold, finite-size scaling, car parking problem

1. Introduction

Flow of suspended particles in porous media plays an important role in a number of industrial and natural processes [1]. Deep-bed filtration [2, 3, 4], ground water contamination by slowly invading pollutants below waste disposal sites [5] or by migrating bacteria [6] and the formation of river beds [7] may serve as a few examples. Two basic approaches are widely used to model the phenomenon. In the classical engineering approach, the porous medium is treated as a continuum at length scales which are in the range of a representative elementary volume [8]. Then one can write down differential equations for the physical quantities describing the two-phase flow and solve them with appropriate initial and boundary conditions. However, continuum models are not well suited when processes, on a length scale much smaller than the representative elementary volume, cause dramatic changes in macroscopic quantities such as the permeability and the connectivity of the medium. If such phase transitions are likely to occur statistical models built up by microscopic processes may provide a more realistic treatment of the system. As an example, we take the process of the deposition of particles in a porous medium which eventually leads to clogging. We will also demonstrate the effect of small impermeable inclusions on the critical behaviour of the system.

We present here a *simple* statistical model for the clogging of pores which already shows some of the important features of the real process. Starting from the microscopic process of the clogging of one pore, macroscopic results can be obtained by performing many of such processes and calculating the averages afterwards. Thus, a Monte Carlo simulation is a suitable method of investigation.

Sahimi and Imdakm [9] have already noticed that isotropic percolation models cannot be used to describe the flow of resuspended particles since spatial symmetry is broken by the direction of flow. So we employ a directed percolation model [10] which belongs to a different universality class. For a general understanding of statistical models which exhibit phase transitions, scaling laws for physical quantities of every universality class are found and the behaviour near the critical point is governed by universal exponents. These exponents are independent of microscopic details of the system like the type of the underlying lattice.

But for practical engineering applications the non-universal behaviour of a system may be of great importance. For example, the fraction of particles deposited in a filter bed depends strongly on the coordination number of interconnected pores although a variation of this number will not change universal behaviour. The main emphasis in this work is based upon the investigation of non-universal behaviour and the results are occasionally checked against violation of universality.

In the field of hydrogeology, several experiments on a laboratory scale [7, 11] and on a field scale [12] investigating the sedimentation of suspended particles in a porous matrix have already been done. But they were performed under conditions that make it hard to compare their results directly with the simple model presented here. Of greater importance are experiments done by Harvey *et al.* [6] and by Silliman [13]. They measured breakthrough curves of bacteria and small-sized microspheres in macroscopically heterogeneous porous media. Silliman [13] also investigated the spatial distribution of deposited particles but with a relatively low resolution. Experiments which make use of a directed percolation model, to interpret these patterns, are not known to the author. At least on a laboratory scale they could be performed to validate the present model.

This theoretical study was performed to learn more about the functioning of the process that creates the spatial distribution of particles inside a clogged porous medium. Especially, we will address the following questions. Can deposited particles form clusters with fractal properties under appropriate conditions? How do the total number and mass of these particles depend on their own size and on the pore structure? How do small inhomogeneities change the permeability of the medium with respect to particles?

2. Model Setup

Let us consider a column of porous matter with a liquid (or gaseous) current of constant discharge through it. On top of the column, spherical particles of radius R are injected at a fixed position called the origin. They are carried away by the current through the labyrinth made up by the interconnected cylindrical pores until

they reach the outlet at the bottom. The radii r of those cylindrical bonds are distributed homogeneously in space and have a known pore size distribution $\phi(r)$.

We will make now an assumption about the process whereby a particle passes through the labyrinth. It can move from pore to pore until its radius R is larger than the pore radius r. Then it will bridge the pore and rest there forever. It cannot move backwards against the direction of the current. Thus, the flow field is introducing an anisotropy. This shall be by definition the microscopic mechanism for our simulation. The particles cannot interact among themselves if we keep their concentration low. For particle radii larger than 30 μm our assumption is reasonable because pore bridging is the dominant process. Other effects like van der Waals adhesion or chemical reactions do not occur [3].

The probability p that a particle hits a pore for deposition is given by

$$p = \frac{\int_R^\infty \phi(r)\,\mathrm{d}r}{\int_0^\infty \phi(r)\,\mathrm{d}r} \tag{1}$$

and is completely determined by a combination of geometrical properties of the particles and the porous matrix. In accordance with the terminology of percolation theory [4] we call p the occupation probability. Although one may argue that larger pores contain a higher percentage of the fluid flow, Equation (1) is still correct. Pore diameters can be weighted in this way because Equation (1) is looking at all potential trapping locations. This is entirely dependent on spatial properties and, thus, the flow distribution is not important. The pore size distribution can be taken from a measurement. By taking particles with varying radii, p can be tuned experimentally. In our model small particles have a very low chance of deposition. They will therefore reach the outlet at the bottom of the column, whereas large particles cannot intrude into the porous matrix and most of them will rest on top of it. Obviously, there is a critical radius in between where a maximum number of particles will deposit. In this way, the process of deposition is described as a critical phenomenon. In an infinitely large matrix an infinitely large number of particles will deposit when a critical occupation probability or percolation threshold $p_c = p(R_c)$ is reached. This corresponds to the divergence of the mean cluster size S which we define later in Equation (5). The particles with the critical radius R_c then form a cluster with self-similar or fractal properties. Once the pore size distribution and p_c are known, R_c can be calculated from Equation (1) implicitly. Comparing a given particle radius R to R_c can now serve as a criterion to predict fractal pore clogging.

Other quantities like the correlation lengths $\xi_\perp$, $\xi_\parallel$ perpendicular and parallel to the direction of flow are also diverging. The order parameter P_0 is defined as the probability that a cluster stretches from the origin to the outlet. This percolation probability is zero below the critical point. Inside the critical region all these quantities vary as a function of p with power laws and universal critical exponents [14].

Hence, we get

$$\begin{aligned} &S \sim \mid p - p_c \mid^{-\gamma}, \\ &\xi_{\perp,\parallel} \sim \mid p - p_c \mid^{-\nu_{\perp,\parallel}}, \\ &P_0 \sim (p - p_c)^{\beta} \quad \text{for} \quad p \geqslant p_c. \end{aligned} \tag{2}$$

Universality is independent of the chosen lattice type and holds for each dimension if perturbations to the system remain irrelevant (cf. [15, 16] and references therein).

For practical reasons we perform the calculations in two dimensions and reshape the column into a thin slab. We map the positions of the pore centres on lattice points of a square lattice and the direction of flow is along the square diagonals. To the lattice we apply the rules of directed site percolation [10]. For the $2d$ case, the percolation threshold and the critical exponents have been deduced accurately from a series expansion [17]

$$\begin{aligned} &p_c = 0.705489(4) \\ &\gamma = 2.278(2), \qquad \nu_{\perp} = 1.097(2), \\ &\nu_{\parallel} = 1.734(2), \qquad \beta = 0.276(3). \end{aligned} \tag{3}$$

The fractal dimension d_f at the critical point is defined as the exponent of the relation between a characteristic length ξ and the mass S of a cluster. If we take $\xi = \sqrt{\xi_{\perp}\xi_{\parallel}}$ we have

$$S \sim \xi^{d_f} \quad \text{with} \quad d_f = 1.805(2) < 2 \tag{4}$$

in two dimensions [15, 16]. Below p_c the clusters are again fractals but with a lower dimension [14]. Above p_c fractality is maintained in regions smaller than $\xi_{\perp}\xi_{\parallel}$ whereas in larger areas the cluster behaves like a 'massive' object: $S \sim \xi^d$.

Very often the porous matrix appears to be heterogeneous even on the scale of several lattice constants. For example, tight clusters of small impermeable inclusions have been observed in sedimentary rock [18]. We treat them as impermeable inhomogeneities of varying size with a given distribution which are located at random positions. In our model, they block lattice sites which a particle cannot visit while finding its way through the outlet. We first took point-like obstacles shown in Figure 1. They were randomly distributed over the lattice and are taken to be hard so that two of them cannot sit on the same site. Their effect is to reduce the network coordination number locally. A density d for the inhomogeneities is introduced by dividing the number of blocked sites by the total number of lattice sites.

In order to investigate the influence of the obstacle size we looked at horizontal splinters with random spatial distribution. Their length l is measured in diagonal lattice constants and the density d is calculated in the same way as for points. We

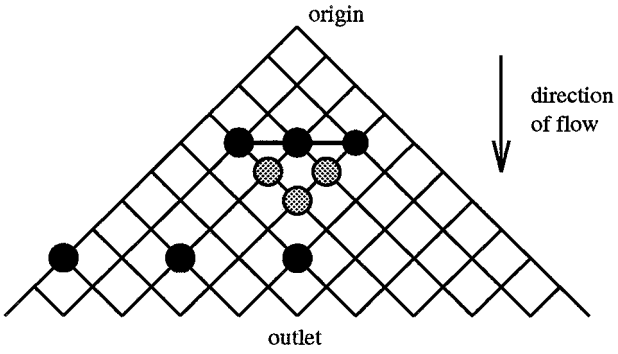

Figure 1. Points (full circles) and horizontal splinters with $l = 2$ (connected full circles) as inhomogeneities on a square lattice, screened sites are grey circles.

choose this shape because it has the largest effect since a maximum number of lattice sites is additionally blocked or 'screened' (Figure 1). Other shapes were found to be less effective, e.g. vertical splinters do not screen at all and therefore act as points.

3. Validity

Setting up a model inevitably requires us to make some simplifications which limit the range of validity. Therefore their implications are discussed below and are compared to more realistic assumptions.

The pore structure is modelled by cylindrical pores connected by nodes. The pore centres are mapped on sites of a square lattice. In reality there are pore necks between nodes, bulges at nodes and the lattice is irregular, e.g. of the Voronoi type. This difference could lead to a shifted percolation threshold. We take a distribution of pore diameters which is homogeneous in space in the unperturbed system. But there may be correlations in the pore structure, e.g. in sedimentary rock which change the permeability [18]. We therefore introduced impermeable inhomogeneities on a microscopic scale. The medium has now undulating correlations of the hard sphere type in it. A system with this kind of inhomogeneities that rest at fixed locations is said to exhibit 'quenched disorder' [19].

The flow and transport process is treated jointly in *one* model of directed site percolation and we always assume the fluid flow and the movement of the particles inside a pore to be from top to bottom. These are drastic simplifications which make it difficult to model time-dependent processes. Since particles do not necessarily fill up all the accessible fraction of the medium it is better to split up the particle movement in three steps. First we have to determine the accessible fraction of the pore space by undirected bond percolation. Then we must calculate the fluid velocity field in the medium. Hereby we obtain an anisotropy which is provided

in this simple model by using directed percolation. By tracking the particles along the flow field we can now bring them to their actual trapping location.

As tracers we use spheres with fixed radius whereas experiments [6, 13] have been done with a size distributed ensemble. These experiments suggest that the clogging mechanism is a combination of mechanical trapping (straining) and adsorption whereas we take pore bridging to be the dominant process.

Nevertheless, it can be argued that even a more sophisticated model would show similar spatial patterns of deposited particles. That means it falls into the same class of universality. Thus, the simplifications place few restrictions on the aim of our investigations.

4. Monte Carlo Simulations

The Monte Carlo simulations were performed with an algorithm for directed site percolation on a square lattice along the diagonal direction [15, 16] which was modified to include the treatment of inhomogeneities. We choose a site on top of the slab as the origin $x = y = 0$ and from there we try to find our way to the outlet at $x = L$. We call the origin 'active' because a particle can sit there and eventually move to the next row. We decide whether a neighbouring site in the next row is active by means of a Monte Carlo step. First we check if the site is blocked by an obstacle. If not, a random number is drawn and compared with the occupation probability p. If it is smaller than p we activate the site, and by reiterating the whole Monte Carlo step we grow a cluster of occupied sites inside a 'light cone' of a 90° opening angle. A light cone is now defined by the area which is occupied by a cluster with $p = 1$. For the directed problem, the probability for a site to become active in row $x + 1$ depends only on its neighbouring sites in row x. To be part of a cluster these sites must be connected to the origin. Five configurations have to be considered to determine whether the site in row $x + 1$ will also be connected. The site percolations are shown in Figure 2.

In a finite-size system the order parameter P_0 is the probability that a cluster grown from the origin reaches the outlet. Such a cluster is called 'infinite'. 'Finite' clusters are those dying before $x = L$. In order to spare computer time the Monte Carlo algorithm ensures that a cluster reaches $x = L$ as fast as possible. This is done by always trying to activate those sites with the largest x-coordinate. The coordinates of sites from which a cluster may eventually grow are stored in a list of active sites. Time is spared because the whole infinite cluster has not been built. Subsequently, if there are no active sites left, a complete finite cluster has been grown. For each value of p we always grow 10^5 clusters in a system of length $L = 1000$ where the total number of lattice sites is $N = 501501$.

Three clusters created with this Monte Carlo algorithm are shown in Figure 3 below, at and above the percolation threshold p_c. Below p_c, the correlation lengths $\xi_{\|,\perp}$ are exponentially small and clusters usually die before they connect to the outlet. At p_c the cluster becomes fractal or self-similar and has holes in it at all

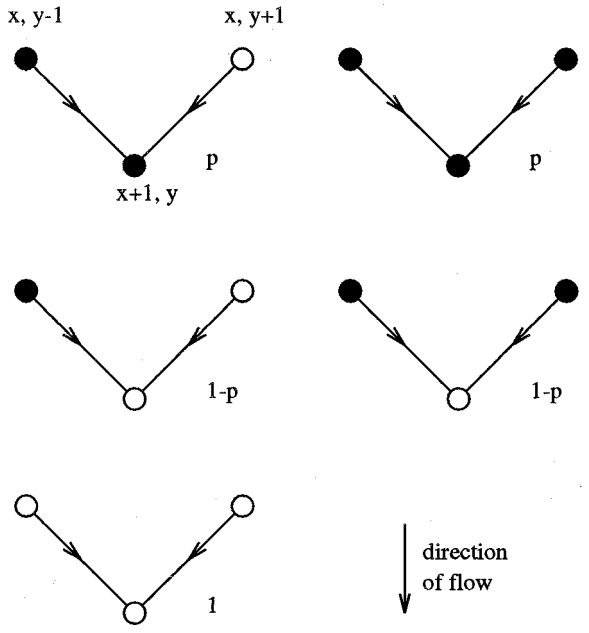

Figure 2. Probability of the site at row $x+1$ to become active (full circle) or not active (circle), sites with full circles are connected to the origin.

length scales. But still it does not extend horizontally in an infinite system since the ratio of the correlation lengths vanishes as $\xi_\perp/\xi_{||} \sim \mid p - p_c \mid^{\nu_{||}-\nu_\perp}$. Large holes disappear for a massive cluster above p_c and it has a finite opening angle. A representative elementary area can be defined in this case if it is larger than $\xi_{||}\xi_\perp$. A cluster now marks the geometric space which is available for the particles. If the cluster is finite (Figure 3(a), (b)) this space can be filled up with particles by stacking them one above another. If it is infinite (Figure 3(c)) there are still some dead end pores where particles will deposit. But with increasing p this number is reduced rapidly and most of the particles reach the outlet.

The obstacles were placed on the lattice with equal probability for each position until the desired density was reached. This was done with an algorithm which is also used for the car parking problem [20]. If part of a splinter fell outside the light cone this part was truncated and excluded from the density calculation. If a length distribution $\Phi(l)$ for splinters was given, the density for a length l was calculated as $d(l) = \int_l^{l+1} \Phi(l')\,\mathrm{d}l'$ with $l = 0, 1, 2, \ldots$ and for $l = 0$ we get points. To obtain the number of splinters of length l we multiplied $d(l)$ with the total number of lattice sites N and made the resulting number an integer. For our value of N this procedure ensures that we get $d = \Sigma_l d(l)$ with an accuracy of at least three digits.

Near p_c and for small obstacles $l \leqslant 5$, it was sufficient to change the spatial distribution after 1000 clusters have been grown. To obtain better statistics at $p \lesssim 1$ for larger obstacles, the distribution was renewed after both 100 and 10 clusters.

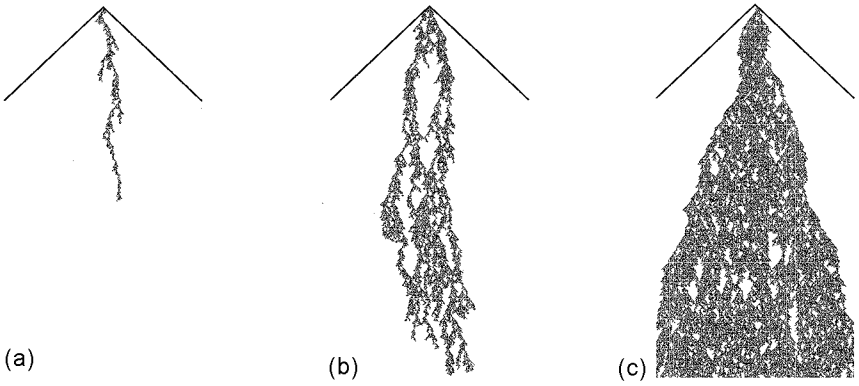

Figure 3. Directed percolation clusters at (a) $p = 0.66$, (b) $p = p_c$, (c) $p = 0.75$ (from left to right) in an unperturbed system with $L = 1000$.

Table I. Number of repetitions of the obstacle distribution (1) near p_c, (2) at $p \lesssim 1$ (for all simulations: system length $L = 1000$, lattice sites $N = 501501$, 10^5 clusters grown).

$d\rightarrow$ $\downarrow l$	0.025	0.05	0.075	0.1
0–5	10^2, 10^2	10^2, 10^2	10^3, 10^4	10^3, 10^4
6–10	10^3, 10^3	10^3, 10^4	10^3, 10^4	10^3, 10^4

Here the fluctuations of the percolation probability P_0 are caused by those of the obstacle distribution. In Table I the simulation parameters are shown schematically. Scanning the region $0.65 \leqslant p \leqslant 1$ with a step length $\Delta p = 0.0025$ meant 140 separate simulations for the calculation of a whole curve $P_0(p)$. Since it took an order of magnitude longer to create a new distribution than to grow a cluster, this was very time consuming especially for higher values of p.

A detailed view of a cluster in an environment of lognormal size distributed splinters, with arithmetic mean μ and standard deviation σ, is given in Figure 4. Because obstacles frequently stop their growth, we must now increase p to obtain infinite clusters. Subsequently, p_c is shifted to higher values. Without obstacles the cluster would be massive but splinters now tear large holes inside. On small areas above a splinter, particles can pile up by forming a massive triangle with no holes in it. Fractal properties now emerge from the interaction between the cluster and the inhomogeneities which are perturbing the system.

In two dimensions the perturbations induced by the inhomogeneities do not change the critical exponents. This can be shown by the replica trick [21] and the perturbations are said to be irrelevant in this case. The method is often

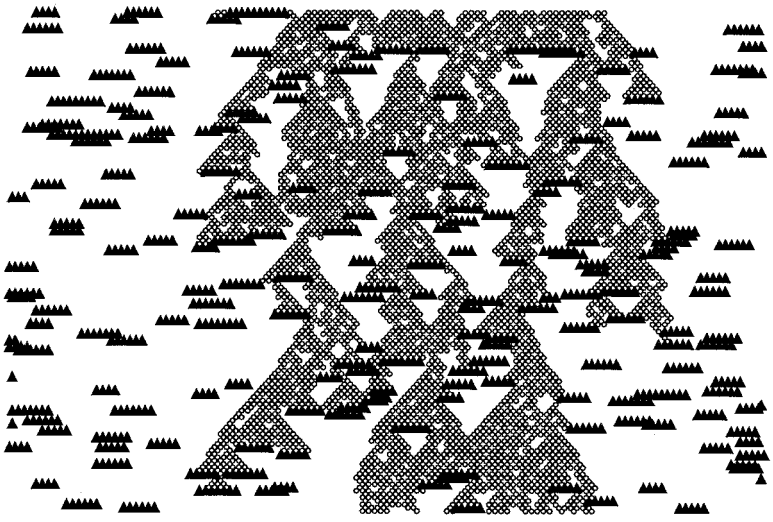

Figure 4. Cluster (circles) between $300 \leqslant x \leqslant 450$ with lognormally distributed splinters (triangles, $\mu = 4$, $\sigma = 1$) at shifted $p_c = 0.808$ and $d = 0.05$.

used in statistical physics to calculate averages of systems which show quenched disorder [19].

To determine the shift of p_c with high precision one has to use the scaling hypothesis [14]. It says that exactly at p_c, the percolation probability varies with the system length as $P_0 \sim L^{\beta/\nu_\parallel}$. At the critical point, a log-log plot of this relation yields a straight line and a linear fit of the Monte Carlo data gives the best result with the lowest error. We performed this fit for various values of the density $d \leqslant 0.1$ and the splinter length $l \leqslant 10$ and found that the exponent ratio $\beta/\nu_\parallel$ was always consistent with 0.159. Usually we used a simpler method to determine the shift. Namely, we looked at the mean cluster size

$$S(p, L) = \sum \frac{n_s s^2}{\sum n_s s}, \tag{5}$$

where n_s is the number of finite clusters of particle number or mass s. At p_c, it diverges according to relation (2). But for finite systems it has its maximum value at $p(L)$ which goes to p_c like $(p(L) - p_c) \sim L^{1/\nu_\parallel}$. We scanned $S(p)$ in steps of $\Delta p = 0.0025$ and took the maximum for p_c with an error bar Δp.

In Figure 5, $S(p)$ is shown for the unperturbed system and for points at different densities. Due to finite-size effects, larger obstacles induce broader maxima and the error was then assumed to be $2\Delta p$. These results were compared for some cases with the values of p_c obtained from the high precision method and were always found to be equal within the error bars. Inspection of additional data shows that the absolute height of the maximum is almost doubled when we keep the density constant and increase the splinter length by ten diagonal lattice constants. This is

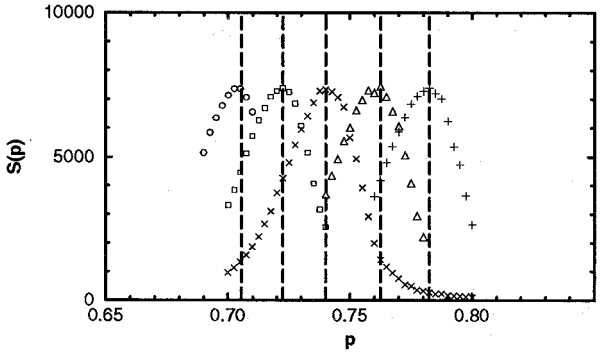

Figure 5. Mean cluster size $S(p)$ of the unperturbed system (circles) and for points with $d = 0.025, 0.05, 0.075, 0.1$ (from left to right).

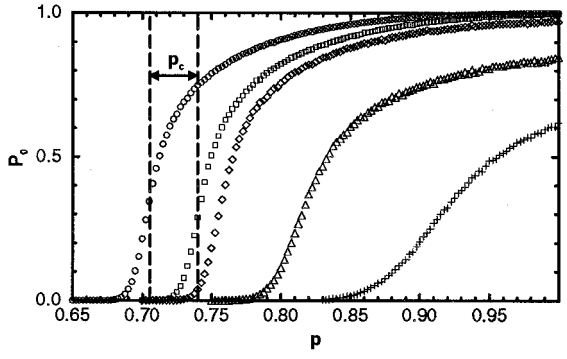

Figure 6. Percolation probability $P_0(p)$ for the unperturbed system (circles) and for splinters at $d = 0.05$ with length $l = 0$ (points), 1, 5, 10 (from left to right).

obviously a non-universal effect but in principle we see that large obstacles force more particles to deposit than small ones.

5. Results

Figure 6 shows the percolation probability $P_0(p)$ for splinters of increasing length at constant density $d = 0.05$. The shifted percolation threshold p_c is $0.740(3)$ for points as indicated. Because finite-size effects are strong P_0 does not vanish at p_c. For the same reason, the slopes of P_0 decrease but it has been checked that the exponents do not change so that universal behaviour is maintained.

Long splinters reduce $P_0(p)$ to less than 1 even if $p = 1$. The areas which consist of a splinter and the screened sites below it (Figure 1) can form percolating clusters which are perpendicular to the direction of flow. They hereby reduce the permeability of the medium even for very large pore sizes and this limit leads to a continuum percolation model for the obstacles.

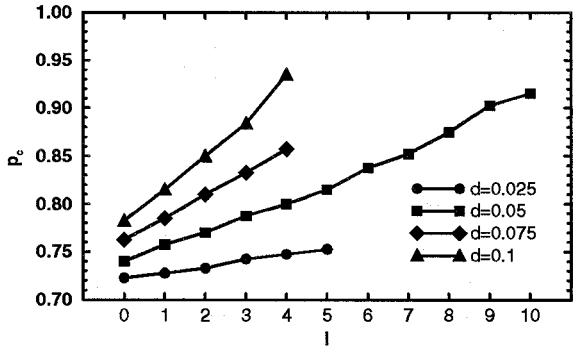

Figure 7. Shifted percolation threshold $p_c(l)$ for different densities d.

To obtain the p_c-shift quantitatively for a wider range a parameters we determined p_c for splinter lengths $l \leqslant 10$ and densities $d \leqslant 0.1$. The shift increases almost linearly with the length as shown in Figure 7. For each curve a linear extrapolation to $p_c = 1$ yields the splinter length $l_{\max}$ where the medium becomes totally impermeable. For the densities $d = 0.025, 0.05, 0.075, 0.1$ the corresponding length $l_{\max}$ is $44, 16, 10, 6$ respectively. Plotting them as a function of d would give a phase diagram separating the permeable phase from the impermeable one. But this would require data for more than four points and is left for future investigation.

The curves in Figure 7 can serve as gauge curves if we want to identify an unknown size distribution $\Phi(l)$ of obstacles. First, we determine the p_c-shift of this distribution $\Phi(l)$. For a given density we can assign to Φ an effective length l_{eff} which we define by the inverse function

$$p_c^{-1}(\Phi) \equiv l_{\text{eff}}. \tag{6}$$

This length dominates the shifting process whereas contributions from larger or smaller splinters in the distribution are less important.

To illustrate the meaning of l_{eff} we determined p_c for four different size distributions of obstacles with the same arithmetic mean μ at $d = 0.05$. The result is shown in Table II. Within the error bars, p_c was always consistent with 0.815 which is the value of splinters with fixed length $l = 5$. From this result we deduce that the shift of p_c is completely determined by the mean μ of the size distribution. Size distributed splinters have the same effect as those with fixed length. Because at the critical point the cluster is a fractal it does not feel variations in the size of splinters. Only the number of blocked sites and therefore the density d induce the p_c-shift. Thus, the results of Table II are explained by the self-similarity of clusters at p_c.

Furthermore, Figure 8 illustrates that not only at p_c but in the whole range $p_c \leqslant p \leqslant 1$ the percolation probability $P_0(p)$ is almost identical for size distributed

Table II. Numerical values of p_c for four obstacle size distributions at density $d = 0.05$.

μ	σ	Type	p_c
5.0	3.16	lognormal	0.818(3)
5.0	3.16	even, $h(0) = \cdots = h(10) = 1/11$	0.820(5)
5.0	5.0	lognormal	0.813(5)
5.0	5.0	peaked, $h(0) = h(10) = 1/2$	0.813(3)
		$l = 5$	0.815(3)

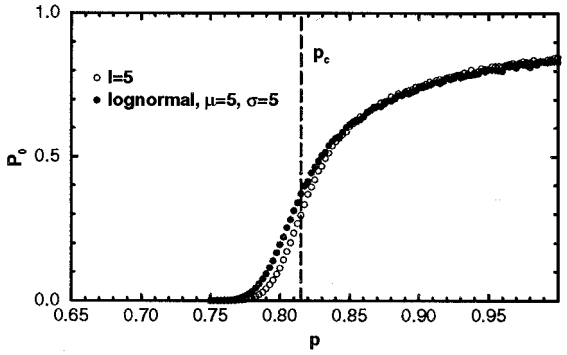

Figure 8. Percolation probability $P_0(p)$ for splinters with length $l = 5$ and lognormally distributed length with $\mu = 5$, $\sigma = 5$.

splinters and for those with fixed length. This result is somewhat unexpected. Obviously, outside the critical region the tendencies for long splinters to increase and for short splinters to decrease $P_0(p)$ are just neutralized.

6. Conclusions

We have described the process of pore clogging by large particles in a porous medium by directed percolation. Due to the anisotropy introduced by the direction of flow this process belongs to a class of universality different from normal random percolation.

Assuming mechanical trapping for large particles ($> 30\,\mu$m), the accessible fraction of the medium has been identified to be a directed percolation cluster. We have varied the radius of the migrating particles and the spatial pattern of this fraction experienced a phase transition. The medium was permeable only for small particles whereas for particles with a radius larger than a critical radius R_c it became impermeable. Sakthivadivel (1972) [11] already observed this type of radius experimentally, but for size distributed particles in a porous matrix with a regular lattice structure. Also Silliman [13] reported that larger particles deposit

with a higher probability. He found the trapping mechanism to be a combination of adsorption and straining for particles $> 7\ \mu$m in a bed of glass beads of the size of several millimetres.

In our model, the deposited particles of the critical size form a cluster with fractal properties and their total number is maximal. Taking smaller radii this number should decrease. But this is not true in reality because small particles are adsorbed at pore surfaces [6, 13]. Nevertheless, an experimentally observed fractal structure of deposited particles would support the relevance of a percolation model. It would reflect the disorder of the medium as seen by particles of a particular size.

Winterfeld *et al.* [22] found that the percolation threshold is indistinguishable for a regular honeycomb lattice with coordination number 3 and a lattice built up by random Voronoi tessellation. A similar result for directed percolation may be expected. Note, that in this case we can calculate R_c from Equation (1) for a given pore size distribution. We have now a criterion at hand to predict fractal pore clogging.

The system was no longer spatially homogeneous after we introduced impermeable inhomogeneities of the size of several lattice constants. Because they acted like hard spheres they affected correlations in the pore space. They also shifted the percolation threshold p_c to higher values and thereby reduced the permeability. This behaviour had already been suggested by Thompson *et al.* [18] for certain types of sandstone. Our results also indicate that large obstacles cause more particles to deposit than small ones if we keep their densities constant. This is due to the increased screening effect of large obstacles (Figure 1).

For size distributed obstacles, the mean of the distribution was the only parameter that determined the shift of the percolation threshold for all values of the occupation probability p. Surprisingly, this result holds even *outside* the critical region for $p \lesssim 1$. Here the spatial extension of the obstacles which is characterized by the standard deviation should play a role because the percolation clusters are no longer fractals.

Further investigations should involve three dimensions. Clearly, we then have to deal with another universality class of directed percolation. Microscopic obstacles may even shift the corresponding exponents continuously if the perturbations are relevant for the system [15,16]. Dealing with such behaviour would complicate the analysis considerably compared to the $2d$ case.

Acknowledgements

The author would like to thank L. Turban and W. Kinzelbach for fruitful discussions.

References

1. Sahimi, M., Gavalas, G. R. and Tsotsis, T.T.: 1990, Statistical and continuum models of fluid-solid reactions in porous media, *Chem. Eng. Sci.* **46**, 1443–1502.

2. Kaye, B. H.: 1994, *A Random Walk through Fractal Dimensions*, Weinheim, VCH Verlagsgesellschaft, Chapter 6.
3. Herzig, J. P., Leclerc, D. M., Le Goff, P.: 1970, Flow of suspensions through porous media – Application to deep filtration, *Industr. Eng. Chem.* **62**(6), 8–35.
4. Tien, C. and Payatakes, A. C.: 1979, Advances in deep-bed filtration, *AIChE J.* **25**, 737–759.
5. Haberlandt, R., Heybey, J., Schmid, H. and Vörtler, H.-L.: 1993, Statistical and geometrical modelling of transport and storage behaviour in underground matter of waste disposal sites – III. Computer simulations of disordered and microfractured matter, Statusbericht zum BMFT-Forschungsorhaben 'Deponieuntergrund', Teilprojekt 34, GC 6.
6. Harvey, R. W., Kinner, N. E., MacDonald, D., Metge, D. W. and Bunn, A.: 1993, Role of physical heterogeneity in the interpretation of small-scale laboratory and field observations of bacteria, microbial-sized microsphere, and bromide transport through aquifer sediments, *Water Resour. Res.* **29**(8), 2713–2721.
7. Schälchli, U.: 1993, Die Kolmation von Fliessgewässersohlen, in D. Vischer (ed.), *Versuchsanstalt für Wasserbau, Hydrologie und Glaziologie der Eidgenössischen.* Technischen Hochschule Zürich, Mitteilungen, **124**.
8. Bear, J. and Bachmat, Y.: 1991, *Introduction to Modeling of Transport Phenomena in Porous Media*, Dordrecht, Kluwer, Chapter 1.2.
9. Sahimi, M. and Imdakm, A. O.: 1991, Hydrodynamics of particulate motion in porous media, *Phys. Rev. Lett.* **66**, 1169–1172.
10. Kinzel, W.: 1983, Directed percolation, *Ann. Israel Phys. Soc.* **5**, 425–445.
11. Sakthivadivel, R.: 1972, Sediment transport through a porous column, in: H. Wen Shen (ed.), *Sedimentation, A Symposium in Honour of Prof. H. A. Einstein*, pp. 26.1–26.17.
12. Geldner, P.: 1981, Deterministische und stochastische Methoden zur Bestimmung der Selbstabdichtung von Gewässern, Institut für Wasserbau der Universität Stuttgart, Mitteilungen, **49**.
13. Silliman, S. E.: 1995, Particle transport through two-dimensional, saturated porous media: influence of physical structure of the medium, *J. Hydrol.* **167**, 79–98.
14. Stauffer, D. and Aharony, A.: 1994, *Introduction to Percolation Theory* (2nd edn, rev.), London, Taylor and Francis.
15. Kaiser, C. and Turban, L.: 1994, Fractal dimensions of confined clusters in two-dimensional directed percolation, *J. Phys. A: Math. Gen.* **27**, L579–L583.
16. Kaiser, C. and Turban, L.: 1995, Surface shape and local critical behaviour in two-dimensional directed percolation, *J. Phys. A: Math. Gen.* **28**, 351–363.
17. Essam, J. W., Guttmann, A. J. and De'Bell, K.: 1988, On two-dimensional directed percolation, *J. Phys. A: Math. Gen.* **21**, 3815–3832.
18. Thompson, A. H., Katz, A. J. and Krohn, C. E.: 1987, The microgeometry and transport property of sedimentary rock, *Adv. Phys.* **36**, 625–694.
19. Mezard, M., Parisi, G. and Virasoro, M. A.: 1987, *Spin Glass Theory and Beyond*, Singapore, World Scientific, Chapter 1.
20. Evans, J. W.: 1993, Random and cooperative sequential adsorption, *Rev. Mod. Phys.* **65**, 1281–1329.
21. Turban, L.: 1994, private communication.
22. Winterfeld, P. H., Scriven, L. E. and Davis, H. T.: 1981, Percolation and conductivity of random two-dimensional composites, *J. Phys. C: Solid State Phys.* **14**, 2361–2376.